IEEE Access
Multidisciplinary ⋮ Rapid Review ⋮ Open Access Journal

Received May 7, 2021, accepted June 12, 2021, date of publication June 15, 2021, date of current version June 23, 2021.

Digital Object Identifier 10.1109/ACCESS.2021.3089670

Automatic Identification Algorithm of the Rice Tiller Period Based on PCA and SVM

YUANQIN ZHANG, DEQIN XIAO, AND YOUFU LIU
College of Mathematics Informatics, South China Agricultural University, Guangzhou 510642, China

Corresponding author: Deqin Xiao (deqinx@scau.edu.cn)

This work was supported in part by the Key-Area Research and Development Program of GuangDong Province, China, under Grant 2019B020214002, and in part by the Science and Technology Program of GuangZhou, China, under Grant 201904010196.

ABSTRACT The tillering period of rice is the crucial phenological period for the cultivation of high-quality and high-yield rice. Currently, human inspection is mainly used for identification, but it is time-consuming, laborious, and prone to mistakes. To efficiently and accurately identify the start date of rice tillering in the monitoring area, this paper proposed a new algorithm called rice tiller period recognition combining principal component analysis (PCA) and a support vector machine (SVM) (RTR-CPS). This algorithm characterizes the problem of identifying the rice tiller stage as a binary classification problem of rice either entering or not entering the tiller stage. To improve the image segmentation quality of traditional visual segmentation methods, the algorithm was designed to extract five image feature values to describe the rice tiller stage in a multi-featured way, reducing the impact of single feature value bias on the identification of the rice tiller stage. To improve the performance of the rice tiller stage recognition model, the algorithm selects ideal principal features in limited sample data by the PCA algorithm and optimizes SVM classification model hyper-parameters by combining 5-fold cross-validation. The experimental results showed that the accuracy of the algorithm for identifying the tillering date of potted rice was as high as 97.76%, which is significantly higher than other competitive methods, and the maximum error between the detection results and human inspection of potted rice tillering period was no more than 2 days. The rice tillering stage recognition model was applied to the field, and the images of field rice planted by two different methods were tested, which verified that the algorithm proposed in this paper is generalizable. These results fully demonstrate the feasibility and superiority of the algorithm in this paper.

INDEX TERMS Tiller recognition, rice phenology, machine learning, principal component analysis, support vector machine.

I. INTRODUCTION

The improvement of rice yield and quality has always been the focus of strategic agricultural development. Observation of the rice development period is significant to effectively improve the growth management of rice. Each development period's time record can guide farmers to engage in fertilization, irrigation, pest control, and other agricultural activities to cultivate high-yield and high-quality rice [1]. Among them, the rice tillering period is accompanied by the growth stages of roots, stems, and leaves. It is the main period of rice vegetative growth and a critical development period that determines the number of rice panicles [2]. According to the ''Regulations for Agricultural Meteorological Observations'' (hereinafter referred to as the ''standards''), a plant is considered to have entered a developmental stage when a developmental feature appears. The morphological feature that defines the tillering stage of rice is the leaf sheath revealing the tip of the newly formed tiller, and the tip of the leaf is approximately 0.5-1.0 cm in length. The rice population enters the developmental period, determined by the observed total number of plants entering the developmental stage as a percentage of the number of plants, recorded as a whole number, the decimal rounded off, the first time greater than or equal to 10% for the beginning of development [3].

The observation of the tillering stage of rice has been mainly achieved by human inspection. Du *et al.* [4] and Chen [5] indicated that the observation and recording of rice developmental stages requires the observer to follow ''standard'' criteria carefully and to have some basic knowledge

The associate editor coordinating the review of this manuscript and approving it for publication was Jiankang Zhang.

of agriculture, but because there is no fixed reference sample, the actual observation is somewhat subjective, and the recording of developmental stages often varies from person to person. Huang and Huang [6] and Jiang *et al.* [7] revealed that the total number of plants to be observed at the rice tillering stage should be 100, that is, 25 plants per site, and that observations are generally made every two days, on alternate days or on both days. According to the ''standards'' and related literature, the human inspection method is based on visual and instrumental measurements (e.g., the cursor caliper to measure the leaf tip length) in the field to calculate the percentage of plants reaching the developmental period as defined and described in the ''standards''. In long-term observation practice, human inspection methods are time-consuming, labor-intensive and prone to large human errors. Human inspection also causes contact damage and results in discontinuous observations. Therefore, traditional human inspection methods barely meet the needs of agricultural modernization, and there is an urgent need to study automatic observation methods of the rice tillering stage to reduce labor costs, improve accuracy and real-time observations, and avoid damage to the plant.

Modern agricultural production relies on automatic observation of crop development. Automatic observation methods are mainly divided into two categories based on the sensor platform used. The first category is the remote sensing (RS) monitoring method, including satellite platforms and unmanned armed vehicle (UAV) platforms. Remote sensing techniques are suitable for macroscopic monitoring of crop growth status [8] and crop classification identification [9]. at large scales. Several studies have demonstrated the potential of multi-temporal remote sensing data for monitoring the phenology of crops, such as rice [10]–[14], wheat [15] and forests [16]. The second category uses digital cameras to monitor and continuously obtain sequential images of the ground. These platforms use image processing methods to reflect the phenotypic characteristics of vital crop developmental periods [17], [18].

Although there has been some research on RS for detecting crop development, there is no substitute for ground-based observations of crop development; for example, observing gradual crop development, such as rice tillering, is difficult to achieve using remote sensing technology. RS technology has a long imaging distance and low resolution and is suitable for large-scale analysis of crop growth; however, RS technology is unsuitable for continuous observation. In contrast, daily ground observations can continuously observe the growth status of crops in a small area [19]. In the crop growth process, key crop development periods can be determined by observing changes in the phenotypic characteristics of the crop. For example, Yu *et al.* [20] used a novel crop segmentation method to automatically detect the seedling and three-leaf corn stages. Hufkens *et al.* [21] and Zhu *et al.* [22] used smartphones to take farmland images and used computer vision technology to detect when wheat heading began. Guo *et al.* [23] used a time series (every 5 minutes from 8:00 to 16:00) of RGB images obtained in the field to automatically characterize rice flowering dynamics. Bai *et al.* [24] used a support vector machine (SVM) and diffusion-convolutional neural networks (DCNNs) to distinguish image patches of rice ears. The number of spikes detected determined the heading date of the rice. Han *et al.* [25] used images from a handheld camera to detect rice phenology in real time through convolutional neural networks (CNNs).

Accurately distinguishing the rice in the monitored area from the background before the phenotypic features of the rice tillering stage are translated into image features is a key aspect of effectively identifying the tillering stage. Vision-based segmentation of green crop images is mainly based on thresholding [26], [27] clustering [28], [29] and edge [30], [31] segmentation algorithms. Although traditional vision image segmentation algorithms do not have the universality of deep learning segmentation algorithms, they can reduce the cost of data annotation and are simpler to design for specific problems.

After rice leaf segmentation was completed, the phenotypic characteristics of the rice tillering stage were transformed into image features to determine whether the rice had reached the tillering period. Currently, the essence of identifying the rice tillering period is that the rice has not entered the tillering stage or the binary classification problem under the mode of entering the tillering stage. Therefore, it is appropriate to characterize the rice tillering stage identification problem as a binary classification problem.

Image classification is a basic task in computer vision. With the development of computer vision technology, image classification using traditional machine learning and deep learning algorithms has become a popular research focus. This is because compared with earlier traditional image classification methods [32], [33], image classification methods of traditional machine learning and deep learning use computers to analyze data, find rules from known data, and analyze unknown data using these rules [34]. The difference is that deep learning image classification algorithms use convolutional neural networks (CNNs) to automatically extract image features [35]–[37], while traditional machine learning algorithms require prior knowledge to self-construct and extract image features and then use the classifier to obtain classification results [38]–[41]. However, the deep learning model with a small amounts of data is very easy to over-fitting and performs poorly. This is because the deep learning algorithm can be regarded as a feature learner, which requires a large amount of data to adequately learn the features contained in the image [42]–[44]. The number of rice images obtained in this paper is limited, and no publicly available data have been found; thus, to a certain extent, application research of the deep learning model is difficult. Therefore, this study proposes a new method to identify rice tiller period based on domain knowledge for feature modeling, which enables high-precision identification of the rice tiller period with a limited number of samples.

This article is organized as follows: This paper introduces the image acquisition method and automatic recognition algorithm of rice tillering period in section II (materials and methods). This section introduces a two-stage rice leaf image segmentation method based on the visual image segmentation technique. Based on this, multiple image features were extracted to describe the rice tiller period, and data dimension reduction was performed through the PCA algorithm to reduce the number of features and select the best features. Then, the best features and optimized SVM model were integrated to construct the rice tillering period identification model. In section III, based on the image sequence before and after the rice tillering period, the constructed rice tilling stage recognition model was tested and analyzed. Experiments had fully proved the superiority and generalization of the algorithm proposed in this paper. Finally, the summary and the outlook for future research work in section IV.

II. MATERIALS AND METHODS

A. IMAGE DATA ACQUISITION

In this paper, the selected rice variety was 'Jinnongsimiao'. Rice was planted in pots with a diameter of approximately 40 cm. Seedlings were planted in three holes in each pot, and the seedlings were separated by approximately 10-12 cm. A total of 18 pots of rice were planted in the experiment, with the same interval and density of planted rice in each pot. However, the pots were divided into two areas and monitored by two cameras on the left and right. The 9 pots of rice in each monitored area were arranged in 3 rows and 3 columns, simulating a block of real rice fields.

The nitrogen level of rice in both monitoring areas was N180, which is within the normal range for rice grown at nitrogen levels. The video camera model was a Hikvision DS-2DC4420IW-D smart dome (the camera can adjust the scope of the monitoring area by adjusting the focus), both fixed on a beam 2.5 m above the ground. Only 9 pots of rice were placed in the field of view of each camera for monitoring because more pots would be beyond the field of view. There were basically no differences between the images captured by the two cameras, which were set up to increase the data set and help improve the performance of the training model. In addition, when testing, capturing images on two cameras is equivalent to repeating the experiment during the same period, which can verify the reliability of the results and reduce experimental error. The specific laboratory equipment and site layout are shown in Figure. 1.

Time-lapse shooting of the above-potted rice before and after the late rice tillering period was carried out for the two phases in 2020 (July 22nd-August 02 for the first phase, October 23rd-November 3rd for the second phase). The capture time was set to take an image on the hour between 8:00-17:00 every day, and images were automatically saved to the network hard disk. The size of each captured image was 1920 × 1080 pixels, stored in JPG format. During the experiment, four time series images were obtained (the first phase of the left camera was sequence 1, the second phase of the left camera was sequence 2, the first phase of the right camera was sequence 3, and the second phase of the right camera was sequence 4). There were 120 images in each phase, with a total of 480 images.

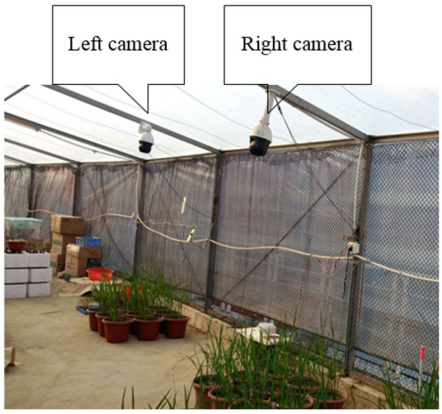

FIGURE 1. The laboratory equipment and site layout in this study.

B. RTR-CPS ALGORITHM DESCRIPTION

Rice tiller period recognition combining PCA and SVM (RTR-CPS) algorithm mainly includes four stages: a two-step method to accurately segment rice leaves, extraction of tillering stage feature values, construction of rice tillering stage detection models, and identification of the rice tillering period. The RTR-CPS algorithm flow is shown in Figure. 2.

Stage 1: A two-stage image segmentation method based on color features was designed. First, the original image was roughly segmented to eliminate the background area with a large color difference from the rice leaves to obtain an image with only rice leaves and moss. Second, the image with only rice leaf was obtained by further fine segmentation to eliminate moss.

Stage 2: Multiple feature values characterizing the rice tillering stage were extracted. Extraction of multiple feature values was performed based on binary images of all rice leaves: leaf coverage, maximum connected area, number of connected points and number of trigeminal points and endpoints of the skeleton. These feature values were preprocessed together to form sample data that were used to train or test the model.

Stage 3: An effective useful rice tiller stage detection model was established by combining principal component analysis (PCA) and the SVM algorithm. The necessary steps of the detection model were as follows:

- The normalized raw sample data were randomly divided into training and test sets, with 70% of the images (336 images) being randomly selected as the training set and the remaining 30% (144 images) being randomly selected as the test set.
- PCA dimensionality reduction was performed on the sample data to calculate the principal component matrix and the principal component contribution rate.

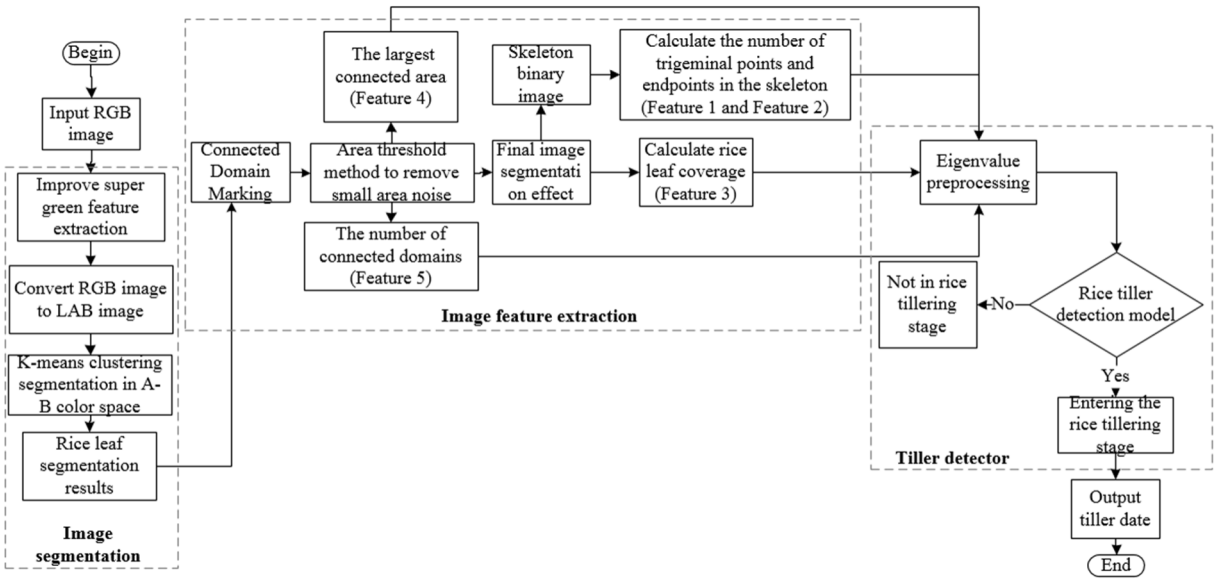

FIGURE 2. The algorithm flow chart.

- The principal element feature combinations were selected according to the principle of increasing cumulative contribution rates to optimize the SVM classification model hyper-parameters.
- Ideal principal element combinations were selected using the training set to build a rice tillering stage detection model.
- Testing was performed using the test set, and the results were analyzed and evaluated.

Stage 4: Online continuous acquisition of time-series-based rice images was conducted. The average feature value of all images per day was calculated and fed into the rice tiller stage detector for rice tiller period identification, and the start date of the rice tiller stage was the output.

C. THE TWO-STAGE IMAGE SEGMENTATION METHOD

1) COARSE SEGMENTATION WAS PERFORMED BASED ON THE IMPROVED EXCESS GREEN FEATURE

When segmenting crop plants from the background, differences in color characteristics can be used. Under different lighting conditions, the R, G, and B values of each pixel of the RGB image will also change accordingly, so the RGB component values cannot be used directly for segmentation. Using simple linear combinations, such as the excess green (ExG=2G-R-B) feature to form relative color factors, can significantly reduce the impact of light intensity or shadows and is often used to segment green crops and backgrounds [45].

In this study, the background of rice leaves included the ground, the flowerpot, soil, the water surface, shadows, and moss. Except for moss, the color information of other background objects and the leaf surface are quite different. The threshold segmentation method of the excess green feature is considered to eliminate other background objects. However, because the rice leaf surface is thin and the background information is complex, the traditional ExG feature segmentation effect is not ideal. The segmentation result is much larger than the rice area in the original image. Many experiments have revealed that when the G coefficient is different, the results of image segmentation are very different, so segmentation effect analysis shows that if the segmentation result is larger than the rice area in the original image, it is under-segmented. The coefficient should be reduced until a particular area of the rice leaf surface in the original image disappears or is divided into two or more areas (red circle mark), which is called over-segmentation. The results show that the third test is the best, and the G coefficient is 1.6. As shown in Figure 3, the improved ExG feature image can sufficiently suppress the background information and preserve the foreground rice leaf surface details.

2) FINE SEGMENTATION WAS PERFORMED BASED ON K-MEANS CLUSTERING

The region of the original image after rough segmentation contains background moss and the rice leaf surface in the foreground (Fig. 4a), which needs further fine segmentation to extract the rice leaf surface. In this study, a method of rice leaf surface extraction in LAB color space was proposed. The image was transformed from RGB space to LAB space (Fig. 4b), and A-B components were extracted. The K-means clustering algorithm combined with the histogram peak number was used to segment the image, which can segment the moss (Fig. 4e) and the rice leaf (Fig. 4f) to achieve more accurate image segmentation. In this study, the default Euclidean distance of the K-means clustering algorithm was used as the similarity calculation method. The peak partition method of the A-B component histogram (Fig. 4c) was used

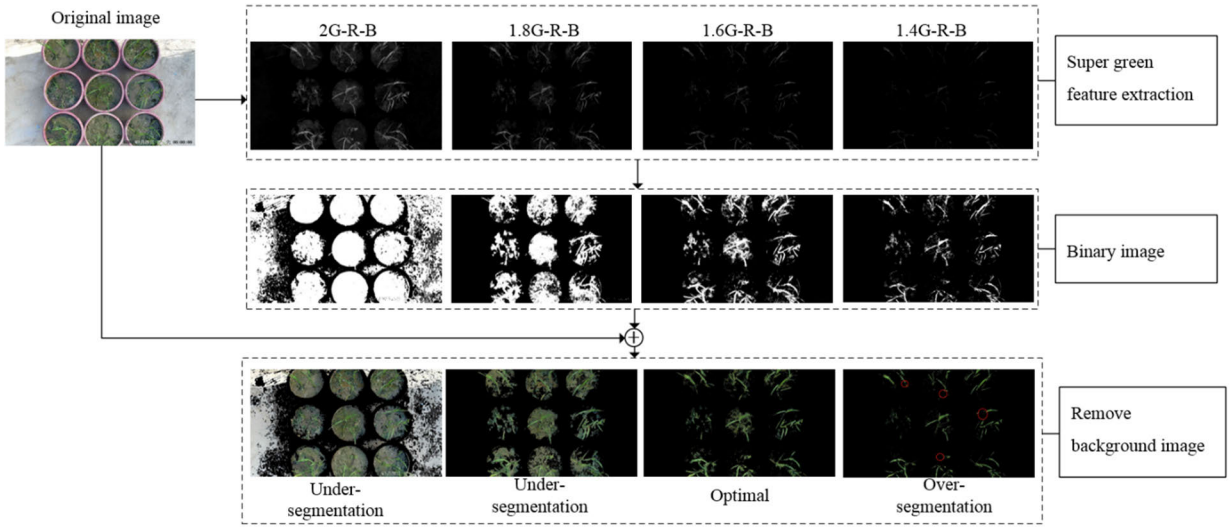

FIGURE 3. Coarse segmentation for removing background.

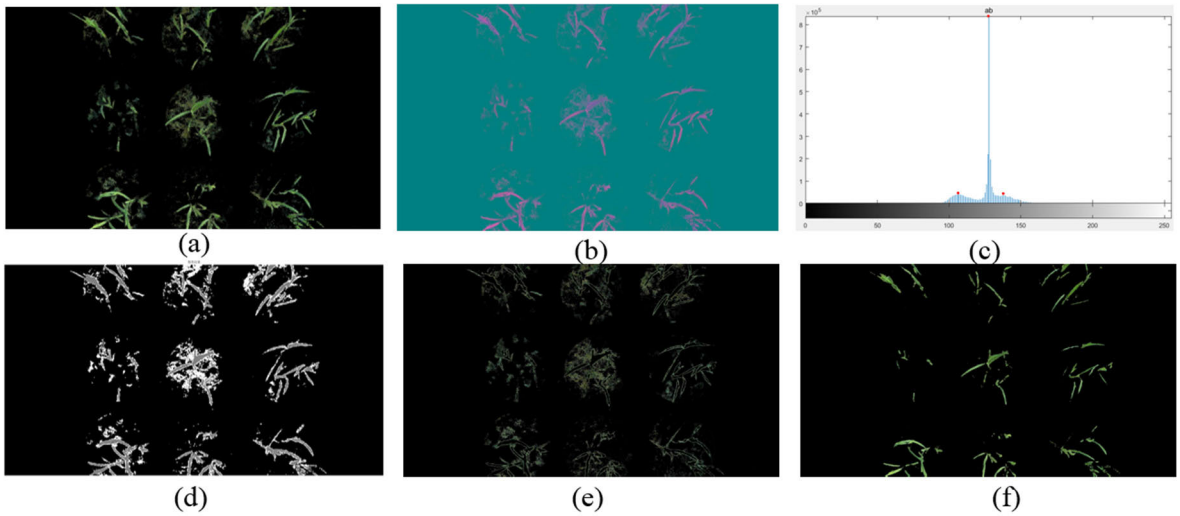

FIGURE 4. Fine segmentation processing. (a) RGB image after rough segmentation; (b) LAB image after rough segmentation; (c) A-B component histogram; (d) image marked with clustering index; (e) background moss after fine segmentation; (f) foreground rice leaf surface after fine segmentation.

to select the cluster number k as 3, and the pixels were marked with a cluster index (Fig. 4d). Figure 4 shows the K-means clustering segmentation process based on the A-B color space.

D. EIGENVALUE EXTRACTION FOR THE RICE TILLERING STAGE

Rice tiller means that new tiller leaf tips emerge in the leaf sheath after the rice turns green. The most apparent feature of rice entering the tillering period is the increase in stems and leaves caused by tillering. Through comparative analysis of the rice leaf image segmented before and after rice tillering, the coverage of the rice leaf surface in the image will roughly increase with the growth and development of the rice, especially when it enters the tillering period. This is a relatively intuitive rice tiller characteristic. However, the rice image segmentation algorithm proposed in this paper cannot eliminate illumination, which makes the rice leaf coverage fluctuate. Therefore, this paper selected more image features to describe rice tillers and has reduced the influence of the deviation of a single feature on rice tiller identification.

The specific methods of image feature extraction were as follows. First, the connected regions of the finely segmented binary image were labeled. Then, the area threshold method was used to remove the smaller area of the noise to obtain the final image segmentation result. Moreover, the maximum connected region area and the number of connected regions were calculated as the rice tiller stage feature values. These two feature values can reflect the adhesion between plants during rice growth. Conversely, to compensate for the

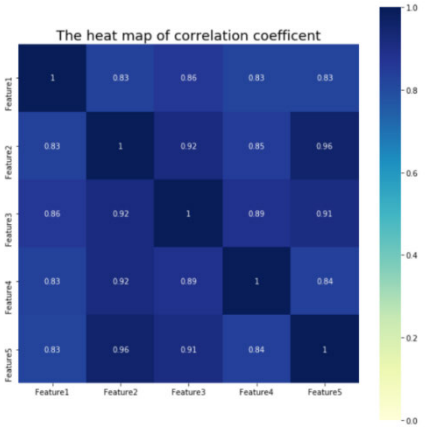

FIGURE 5. Pearson correlation coefficient heat map.

influence of illumination changes on under-segmentation or over-segmentation of the edge of rice leaves in the image, the skeleton binary image of the final segmentation result was extracted using the classic thinning algorithm [46]. Then, the number of trigeminal points and the number of endpoints in the skeleton binary image were calculated, which were also used as the feature values for detecting the rice tiller stage. The trigeminal point refers to the point on the skeleton that satisfies the 3 × 3 neighborhood with two or more bending points, which can reflect the intersection of rice leaves. The endpoint refers to a pixel point on the skeleton branch, which is the tip and tail of the rice leaf, reflecting the number of leaves.

E. CONSTRUCTING A RICE TILLER DETECTION MODEL

1) FEATURE VALUE PREPROCESSING AND CORRELATION ANALYSIS WERE CONDUCTED

In this paper, the detection problem of the rice tillering period is transformed into a two-classification problem, and five feature values of trigeminal points, endpoints, coverage, maximum connected area, and connected number are extracted for each rice image before and after the tillering period. To reduce the impact of rice planting density and image subtitles on the classification algorithm, we divided the feature values of the subsequently obtained rice images by the feature values of the first collected image for preprocessing.

In general, the number of training samples increased exponentially with increasing feature dimensions. Otherwise, over-fitting occurred. However, the number of samples for rice tillering period detection based on four time series images was limited. When the number of features exceeds a certain threshold, the performance of the model may be affected. Figure 5 shows the correlation detection matrix diagram of the feature values extracted from the rice image. The Pearson correlation coefficients in the graph were all higher than 0.8, and the feature information contained from the high correlation feature values was also highly similar. Although the features herein were related to class labels, there was noise and redundancy. In this case, a data dimension reduction method was needed to reduce the number of features, reduce noise and redundancy, and reduce the possibility of over-fitting.

2) DATA DIMENSIONALITY REDUCTION PROCESSING WAS CONDUCTED BASED ON THE PCA ALGORITHM

The purpose of using PCA dimensionality reduction in this paper was to map the original 5-dimensional feature variables into new orthogonal k-dimensional features (where k<5). The new feature data obtained after the PCA dimensionality reduction process reduced the information relevance and redundancy of the original feature variables. The new k-dimensional features are called principal elements and take the form shown in the system of linear Eq. (1).

$$\begin{cases} F_1 = a_{11}X_1 + a_{12}X_1 + \ldots a_{15}X_5 \\ F_2 = a_{21}X_1 + a_{22}X_1 + \ldots a_{25}X_5 \\ \ldots\ldots \\ F_k = a_{k1}X_1 + a_{k2}X_1 + \ldots a_{k5}X_5 \end{cases} \tag{1}$$

where F_1 represents the first principal component formed by the first linear combination of the original feature variables (X_1...,X_5). Generally, the first principal component contains the largest amount of information. If the first principal component is not sufficient to represent the information of the original 5 feature variables, then the second principal component is considered, and so on. The principal components are independent of each other. The determination of k in F_1, F_2...F_k is determined by the cumulative contribution rate of variance in Eq. (2). Generally, when G(k) > 85%, it can sufficiently reflect the information of the original characteristic variable, corresponding to the first k principal components.

$$G(k) = \sum_{i=1}^{k} \lambda_i \Big/ \sum_{j=1}^{5} \lambda_j \tag{2}$$

where λ_i (i=1...,k) is the eigenvalue of the first k principal components of the equation system, and the corresponding eigenvector matrix is called the dimensionality reduction transformation matrix. Then, the new k-dimensional principal element features are the left multiplication of the original sample matrix by the reduced dimensional transformation matrix.

3) THE SVM CLASSIFICATION MODEL AND EVALUATION INDICATORS WERE

SVM was formally proposed in 1995 to solve the binary classification problem of small-scale sample training and is a classic representative of supervised learning. SVM has good robustness and strong generalization ability for unknown data. Additionally, SVM has better performance than other traditional machine learning algorithms for small amounts of data. Therefore, this paper used the SVM algorithm as the rice tiller classification model.

The performance of the classification model in machine learning can be characterized by the confusion matrix between the predicted result of the model and the real result.

TABLE 1. Confusion matrix of binary classification results.

Predicted result	Real result	
	Tiller	No tiller
Tiller	TP	FP
No tiller	FN	TN

The confusion matrix definition of the two classification results is shown in Table 1. TP is the number of positive classes judged as positive classes. FP is the number of negative classes judged as positive classes. FN is the number of positive classes judged as negative classes. TN is the number of negative classes judged as negative classes.

The main diagonal position element of the confusion matrix corresponding to a good recognition model is as large as possible, and the other position elements are as small as possible. Based on the statistical results of the confusion matrix, the accuracy was calculated by Eq. (3) to characterize the overall performance of the classification model. The Kappa coefficient [47] was calculated by Eq. (4) to measure the classification accuracy and characterize the classification ability of the model. Larger values are an indication of better classification performance.

$$Acc = \frac{TP + TN}{TP + FP + TN + FN} \tag{3}$$

$$K = \frac{N \cdot \sum_{i=1}^{r} x_{ii} - \sum (x_{i+} \cdot x_{+i})}{N^2 - \sum (x_{i+} \cdot x_{+i})} \tag{4}$$

where K is the Kappa coefficient, r is the number of rows of the confusion matrix, x_{ii} is the value on the i-th row and i-th column (diagonal), x_{i+} and x_{+i} are the sum of the i-th row and i-th column, respectively, and N is the total number of samples.

4) A PCA-SVM-BASED MODEL WAS GENERATED FOR DETECTING THE RICE TILLERING STAGE

The rice tiller stage detection model is a model that combines PCA and SVM. The framework of the rice tiller detection model is shown in Figure 6.

First, five feature values characterizing the tiller stage were extracted from all the rice leaves in the image, and these were preprocessed together to form sample data. In this paper, 27 rice plants were planted in the monitoring area. If 3 or more rice plants were tillering (the tiller percentage reached 10%), the rice in the image had entered the tiller stage, and the sample was marked as '1'; otherwise, the sample was marked as '0'. The sample data with labels were randomly divided into a training set and a test set. Seventy percent of the images (336 images) were randomly selected as the training set, and the remaining 30% (144 images) were randomly selected as the test set.

In the training set, each standardized sample data point was subjected to principal component extraction to generate principal element features with decreasing principal component contribution in order. Then, the principal component feature combination was selected according to the principle of increasing the cumulative contribution rate. Furthermore, the SVM classification model with different kernel functions was used to classify the principal component feature combination to determine whether the rice was tillering and to determine the ideal principal component feature according to the classification effect.

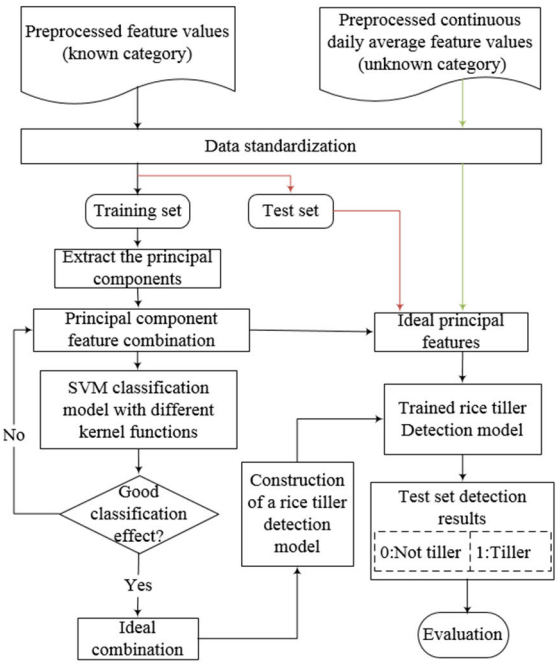

FIGURE 6. Rice tiller stage detection model.

After the ideal principal component features were determined, the training data were randomly divided into five disjoint subsets of the same size. Using the data of the four subsets as the training set and the remaining subset as the verification set, we obtained five groups of training sets and verification sets. The SVM model was optimized by the grid search method to return the optimal hyper-parameter combination that minimized the average error of the five sets of verification results under the two kernel functions.

Finally, a rice tiller detector was constructed by fusing the ideal principal component features and the optimized SVM model. After preprocessing the new test data, the ideal principal component characteristic parameters were extracted as the test set of rice tiller detection to test the classification effect of the trained rice tiller detection model on the new data.

F. IDENTIFYING THE RICE TILLERING PERIOD

This study was based on a time series of rice images to identify the rice tillering period. Specifically, the feature values of the rice images at all times of day were used as the input of the rice tiller stage detection model. Once the detection results of the day and the previous day occurred with a 0-1 ("0" means not in rice tillering stage, "1" means entering rice tillering stage) positive jump, then the output date of the day was the tillering date.

TABLE 2. The eigenvalue and principal component contribution rate calculated by PCA.

Variable	PC1	PC2	PC3	PC4
Eigenvalue	144.595	8.403	2.700	0.371
Principal component contribution	0.901	0.060	0.021	0.011

TABLE 3. A 4-dimensional principal component matrix is obtained by PCA.

Feature	PC1	PC2	PC3	PC4
1	0525	0.677	0.515	-0.028
2	0.183	0.133	-0.389	-0.523
3	0.454	0.151	-0.628	0.613
4	0.674	-0.697	0.224	-0.098
5	0.175	0.123	-0.0373	-0.583

III. RESULTS AND DISCUSSION

A. PRINCIPAL COMPONENT ANALYSIS RESULTS

The PCA algorithm was used to reduce the dimensionality of the preprocessed 5-dimensional data. The eigenvalues (arranged in descending order) and the corresponding principal component contribution rates of the 4-dimensional data are shown in Table 2. Table 3 shows the corresponding matrix composed of 4 eigenvectors, called the 4-dimensional principal component matrix. The number of rows is the number of original features, and the number of columns is the number of principal elements after dimensionality reduction. The data reduced to 4 dimensions are the original sample matrix multiplied by the 4-dimensional principal component matrix. After principal component analysis, the sample data reduced the correlation of feature information and improved the model efficiency.

B. FACTORS AFFECTING THE DETECTION EFFECT OF RTR-CPS

1) THE EFFECT OF THE NUMBER OF PRIMARY ELEMENT FEATURES ON THE DETECTION ACCURACY OF THE RICE TILLERING STAGE MODEL WAS DETERMINED

After the principal components were extracted by PCA, the appropriate principal component features were selected as the input of SVM. To evaluate the influence of the number of principal component features on the classification performance of SVM, four principal component combinations were evaluated in which the number of principal component features was selected as 1, 2, 3, and 4 according to the principle of increasing the cumulative variance contribution rate. Different principal component combinations were input into two types of SVM models of linear kernel function (LKF) and radial basis function (RBF) under the default hyper-parameters for classification detection. According to the classification effect, the relationship between the number of principal component features and the detection accuracy of the default hyper-parameter model was initially established. The red triangle mark indicates the detection accuracy of SVM without PCA dimension reduction. As shown in

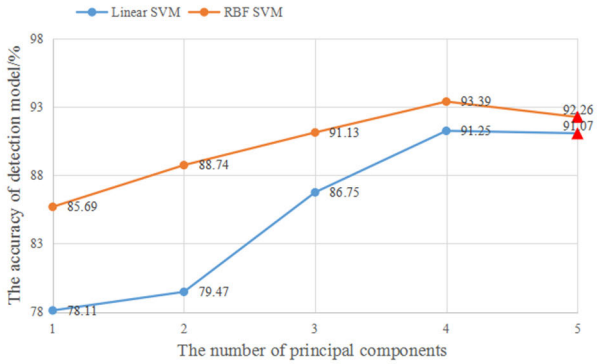

FIGURE 7. The relationship between the number of principal components and the accuracy of the detection model.

TABLE 4. Test results of the rice tillering stage model.

Processing stage	Linear kernel function		Radial basis function	
	Acc (%)	K	Acc (%)	K
Default parameters	91.25	0.685	93.39	0.713
Optimal parameters	94.73	0.802	97.76	0.856

Figure 7, when the number of principal components was 1, the detection accuracy of the two models was low, indicating that it is not reliable to extract only a single feature value to describe the rice tiller characteristics. Both classification models achieved the highest detection accuracy when the number of principal elements was 4. Therefore, it was determined that it was optimal to reduce the number of principal components to 4 dimensions after principal component extraction, at which point the cumulative principal component contribution was as high as 99.5%.

2) THE EFFECT OF OPTIMIZING SVM MODEL HYPER-PARAMETERS ON THE DETECTION ACCURACY OF THE RICE TILLERING MODEL WAS DETERMINED

Table 4 shows the detection results of the SVM model on the test set of extracting ideal principal components at the two processing stages.

Table 4 shows that the accuracy of the RTR-CPS model with the optimal parameters of the LKF and the RBF was significantly better than that with the default parameters. However, the BRF was the best. The Kappa coefficient calculated using different kernel functions corresponding to the optimal parameters increased significantly compared with that of the default parameters, indicating that the hyper-parameters of the 5-fold cross-validation optimization model improved the classification ability of the RTR-CPS model.

C. SUPERIORITY OF THE RTR-CPS ALGORITHM FOR DETECTING THE TILLERING STAGE OF RICE

In this paper, PCA and SVM algorithms were combined to build a rice tiller detection model, and then the test data

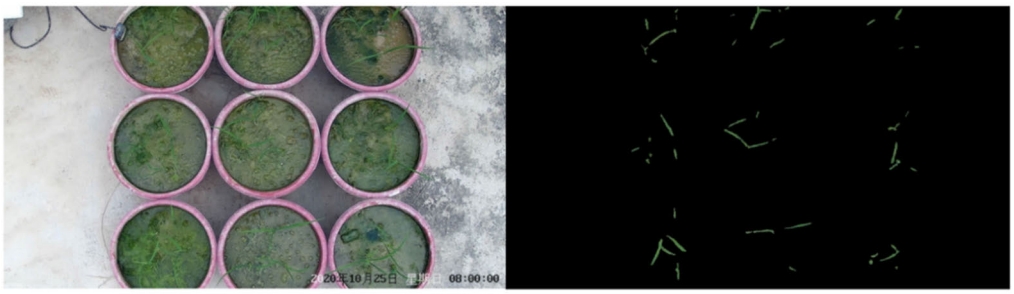

FIGURE 8. Sequence 4 original image and rice leaf segmentation results. (a) sequence 4 original images; (b) the effect of rice leaf segmentation.

TABLE 5. Comparison of model test results.

Model	Common classification algorithm					
	RBF-SVM	KNN	DT	RF	AdaBoost	NB
Without PCA	94.59%	90.07%	88.75%	93.10%	88.81%	89.44%
Fusion PCA	**97.76%**	92.30%	91.68%	92.72%	90.23%	91.99%

TABLE 6. Comparison of automatic detection and human inspection records of the potted rice tillering period.

Image sequence	Human inspection date	Automatic detection date	Error (days)
Sequence 1, the first phase of the left camera	July 27, 2020	July 28, 2020	-1
Sequence 2, the first phase of the right camera	July 27, 2020	July 27, 2020	0
Sequence 3, the second phase of the left camera	October 28, 2020	October 29, 2020	-1
Sequence 4, the second phase of the right camera	October 28, 2020	October 30, 2020	-2

was input after extracting ideal principal component feature parameters to test the trained SVM model. To verify the superiority of combining the PCA and SVM algorithms, as shown in Table 5, the results of the RTR-CPS algorithm were compared with the detection results of other algorithms in the test set.

Table 5 shows that when PCA is not used for data dimensionality reduction, the preprocessed feature values are input into a separate classification model for detection. The RBF-SVM classification model of the optimal parameters was better for processing a small amount of data in this paper. However, the detection accuracy of the RBF-SVM classification model under the optimal parameters is far lower than the detection accuracy of the model proposed in this paper (marked in bold).

When using PCA to extract the ideal principal component features, the detection effect of the classification model changed. For other competitive models, the detection accuracy of the RF model was slightly reduced. However, the detection accuracy of K-nearest neighbors (KNN), decision tree (DT), AdaBoost, and naive Bayes (NB) were greatly improved. Nevertheless, the detection accuracy of other competitive models was still lower than that of the RBF-SVM classification model under the default parameters. This showed that it is necessary to use PCA to reduce the dimensionality of the preprocessed multidimensional data in this paper to eliminate redundancy and noise. In summary, the superiority of this method was verified.

D. RECOGNITION RESULT OF THE RICE TILLERING PERIOD BASED ON THE RTR-CPS ALGORITHM

In this paper, the time series rice images obtained by continuous monitoring were used for classification and detection. The extracted image feature values from each day were averaged before preprocessing, and then the ideal principal component features were extracted and input into the rice tiller detection model. Suppose the detection results of the same day and the previous day have a positive jump from 0-1 (0 represents not in rice tillering stage, 1 represents entering rice tillering stage). In that case, the date of the output is the tillering period. Table 6 shows the comparison results of human inspection and image-based automatic detection of the tillering period of potted rice.

Table 6 shows that the errors of the automatic detection results of the tillering stage of rice in image sequence 1 and sequence 2 corresponding to the first stage of late rice are 1 day and 0 days, respectively, and the average error is 0.5 days. The results of automatic detection of the rice tillering stage of image sequence 3 and sequence 4 corresponding to the second stage late rice were 1 day and 2 days, respectively, with an average error of 1.5 days. Generally, the error between the tillering date detected by this method and the

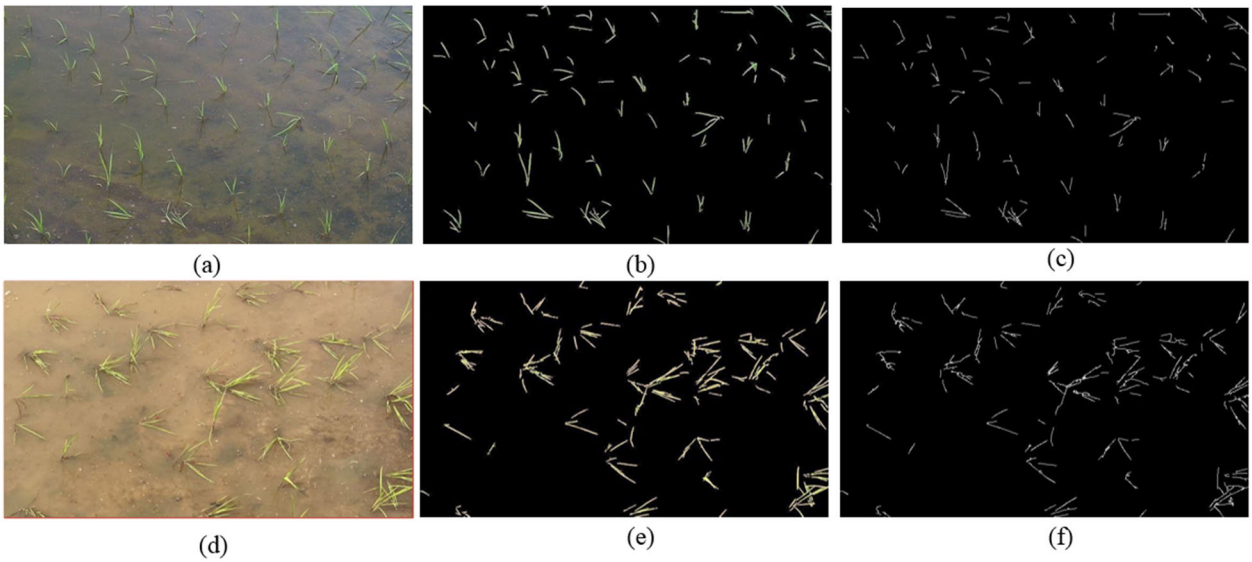

FIGURE 9. Effect images and post-processing results under two surveillance cameras. (a) artificial transplanting seedlings; (b) rice leaves in Fig. 9 (a); (c) skeleton binary image of rice leaves in Fig. 9 (b); (d) artificial throwing seedlings; (e) rice leaves in Fig. 9 (d); (f) skeleton binary image of rice leaves in Fig. 9 (e).

TABLE 7. Classification accuracy of the rice tillering stage model and comparison of automatic detection and human inspection results in field rice.

Monitoring areas	Model classification accuracy	Human inspection date	Automatic detection date	Error (days)
Area (a)	97.32%	April 10, 2021	April 10, 2021	0
Area (b)	95.74%	April 04, 2021	April 05, 2021	-1

observation date is not more than 2 days, and the average error is 1 day. These results show that the automatic detection method is suitable for recognizing the tillering stage of potted rice.

However, the average error of the second stage of late rice is large, which may be due to low temperatures and insufficient light during the second stage of late rice planting, which prevents water evaporation and is conducive to the growth of moss. The proportion of mosses will affect the traditional visual segmentation algorithm designed in this paper to a certain extent, thus reducing the accuracy of recognizing the tillering period. For example, in the image on October 25, 2020, in sequence 4, excessive moss growth in the background led to serious over-segmentation of the rice leaf surface, making the extracted image feature value smaller and resulting in a larger error for the automatic detection of the rice tillering period. Figure. 8 shows the sequence 4 images collected at 8:00 on October 25 and the effect of rice leaf segmentation.

When the background moss grew faster, the coverage ratio was larger, or there was sometimes full coverage. As a result, the influence of the moss was greater, making this method no longer suitable. This is a limitation of traditional visual segmentation methods. Semantic segmentation with deep learning could theoretically be considered to eliminate the effects of moss, but the amount of manual annotation necessary for fine-leaf rice is immense. In fact, from experience, whether in pot or field rice cultivation, growers will actively take various measures to inhibit moss growth and to avoid affecting the growth and development of rice. Therefore, under normal rice growth conditions, this method is efficient and accurate.

E. FURTHER VERIFY THE GENERALIZATION OF THE RTR-CPS ALGORITHM

To verify whether the algorithm proposed in this paper is generalizable, we deployed a field experiment. Two cameras with a resolution of 1280 × 720 pixels were installed in the field to monitor the rice tillering dynamics in two different areas, and 10 images were captured and saved at regular intervals from 8:00-17:00 each day for 15 days (28 March 2021-12 April 2021), with 150 images collected from each field. Fig. 9 shows an example of the results and processing of the images taken under the cameras in the two monitoring areas.

Figure 9 (a) and (d) are the monitoring areas of two different fields. The rice in (a) is planted by artificial transplanting, and the rice in (b) is planted by artificial throwing. Figure 9 (b) and (e) are the rice leaf surfaces obtained by image segmentation in (a) and (d), respectively, and Figure 9 (c) and (f) are the skeleton binary images of (b) and (e), respectively. In this paper, all the image feature values of (a) and (d) for each day were extracted to calculate the average value, preprocessed and extracted from the ideal principal elements and then were input into the rice tillering stage detection model. The results of the classification

accuracy and automatic detection compared to human inspection of the rice tillering model are shown in Table 7.

Table 7 shows that first, the manual seedling throwing planting method in area (b) had a 1.58% lower model classification accuracy than the manual seedling planting method in area (a). The accuracy of both was slightly lower than that of the potted planting method, but both were above 95%. This is because rice in the field is more susceptible to the effects of bad weather, such as rice leaf swaying in the wind and curling when exposed to the sun, which can cause different degrees of variation in the rice leaves under the camera, thus reducing the accuracy of the model classification. Second, the error between the automatic detection date and the human inspection date of rice tillering in areas (a) and (b) are 0 and 1 day, respectively, with an average error of 0.5 days. At the beginning of transplanting, most of the seedlings in area (b) of the artificial throwing planting method showed a dumping posture, and the coverage of the extracted seedlings was larger than that of the other two planting methods. However, after turning green, it will be in a standing posture, which makes the coverage ratio of subsequent images obtained by eigenvalue preprocessing smaller, which introduces errors in the automatic detection of the rice tillering stage. In summary, the experimental results show that the rice tillering stage identification model proposed in this paper can be applied to the field, which verifies that the algorithm proposed in this paper is generalizable.

IV. CONCLUSION AND OUTLOOK

Based on a small sample of images taken before and after the rice tillering stage, this paper proposed an automatic rice tillering stage identification algorithm called RTR-CPS. Experimental results showed that the accuracy of rice tillering stage recognition by this method was 97.76%, which was much higher than that of other traditional machine learning classifiers. The maximum error between the automatic detection results of the tillering period of potted rice and the human inspection date was no more than 2 days, and the average error was 1 day, which shows the feasibility and superiority of this method. Under the conditions of normal growth and rice development, this method is efficient and accurate and can meet the actual needs of agricultural meteorological observation. In addition, we deployed field experiments to verify the generalization of the algorithm proposed in this paper. Future research should include experiments using different camera angles, field late rice, UAV-based image acquisition and other factors to further verify and optimize the algorithm in this paper.

REFERENCES

[1] N. K. Fageria, "Optimal nitrogen fertilization timing for upland rice," presented at the 19th World Congr. Soil Sci., Soil Solutions Changing World, Brisbane, QLD, Australia, Aug. 2010.

[2] R. Q. Zhou and Y. B. Zou, "Lectures on ecological physiology of high yield cultivation of rice (Lecture 12): Life and yield formation of rice," *Hunan Agricult. J.*, no. 12, p. 5, 1996.

[3] W. Yang, *Specifications for Agrometeorological Observation-Rice*. Beijing, China: China Meteorological Administration, 2019.

[4] X. L. Du and F. X. Hu, "Problems and solutions in rice tiller dynamics," *Meteorology*, vol. 31, no. 10, pp. 87–88, 2005.

[5] D. Y. Chen, "Accurate identification and recording of rice developmental stages," in *Proc. 26th Annu. Meeting Chin. Meteorolog. Soc., 3rd Workshop Integrated Meteorolog. Detection Technol.*, 2009, pp. 271–273.

[6] C. H. Huang and Z. L. Huang, "Problems that should be noted in rice observance," *Guangxi Meteorol.*, vol. 23, no. 2, pp. 43–45, 2002.

[7] Y. Z. Jiang, Z. Chen, and X. Ma, "Problems needing attention in agrometeorological observation," *Modern Agricult. Sci. Technol.*, no. 15, p. 338, 2010.

[8] D. Ogawa, T. Sakamoto, H. Tsunematsu, T. Yamamoto, N. Kanno, Y. Nonoue, and J.-I. Yonemaru, "Surveillance of panicle positions by unmanned aerial vehicle to reveal morphological features of rice," *PLoS ONE*, vol. 14, no. 10, Oct. 2019, Art. no. e0224386, doi: 10.1371/journal.pone.0224386.

[9] B. Sapkota, V. Singh, C. Neely, N. Rajan, and M. Bagavathiannan, "Detection of Italian ryegrass in wheat and prediction of competitive interactions using remote-sensing and machine-learning techniques," *Remote Sens.*, vol. 12, no. 18, p. 2977, Sep. 2020, doi: 10.3390/rs12182977.

[10] C. Yu, D. Liu, and Z. Zhang, "Identification of key development stages of rice in Heilongjiang province based on FY-3," in *China Agronomic Bull.*, vol. 30, no. 9, pp. 55–60, 2014.

[11] J. Wang, K. Yu, M. Tian, and Z. Wang, "Estimation of rice key phenology date using Chinese HJ-1 vegetation index time-series images," in *Proc. 8th Int. Conf. Agro-Geoinform. (Agro-Geoinform.)*, Jul. 2019, pp. 1–4, doi: 10.1109/Agro-Geoinformatics.2019.8820262.

[12] Z. He, S. Li, S. Lin, and L. Dai, "Monitoring rice phenology based on freeman-durden decomposition of multi-temporal Radarsat-2 data," in *Proc. IEEE Int. Geosci. Remote Sens. Symp. (IGARSS)*, Jul. 2018, pp. 7691–7694, doi: 10.1109/IGARSS.2018.8517621.

[13] C. Kucuk, G. Taskin, and E. Erten, "Paddy-rice phenology classification based on machine-learning methods using multitemporal co-polar X-band SAR images," *IEEE J. Sel. Topics Appl. Earth Observ. Remote Sens.*, vol. 9, no. 6, pp. 2509–2519, Jun. 2016, doi: 10.1109/JSTARS.2016.2547843.

[14] J. M. Lopez-Sanchez, S. R. Cloude, and J. D. Ballester-Berman, "Rice phenology monitoring by means of SAR polarimetry at X-band," *IEEE Trans. Geosci. Remote Sens.*, vol. 50, no. 7, pp. 2695–2709, Jul. 2012, doi: 10.1109/TGRS.2011.2176740.

[15] A. Burkart, V. L. Hecht, T. Kraska, and U. Rascher, "Phenological analysis of unmanned aerial vehicle based time series of barley imagery with high temporal resolution," *Precis. Agricult.*, vol. 19, no. 1, pp. 134–146, Feb. 2018, doi: 10.1007/s11119-017-9504-y.

[16] S. Klosterman, E. Melaas, J. A. Wang, A. Martinez, S. Frederick, J. O'Keefe, D. A. Orwig, Z. Wang, Q. Sun, C. Schaaf, M. Friedl, and A. D. Richardson, "Fine-scale perspectives on landscape phenology from unmanned aerial vehicle (UAV) photography," *Agricult. Forest Meteorol.*, vol. 248, pp. 397–407, Jan. 2018.

[17] S. Madec, X. Jin, H. Lu, B. De Solan, S. Liu, F. Duyme, E. Heritier, and F. Baret, "Ear density estimation from high resolution RGB imagery using deep learning technique," *Agricult. Forest Meteorol.*, vol. 264, pp. 225–234, Jan. 2019.

[18] A. R. Petach, M. Toomey, D. M. Aubrecht, and A. D. Richardson, "Monitoring vegetation phenology using an infrared-enabled security camera," *Agricult. Forest Meteorol.*, vols. 195–196, pp. 143–151, Sep. 2014.

[19] P. K. Sethy, S. K. Behera, N. Kannan, S. Narayanan, and C. Pandey, "Smart paddy field monitoring system using deep learning and IoT," *Concurrent Eng.*, vol. 29, no. 1, pp. 16–24, 2021.

[20] Z. Yu, Z. Cao, X. Wu, X. Bai, Y. Qin, W. Zhuo, Y. Xiao, X. Zhang, and H. Xue, "Automatic image-based detection technology for two critical growth stages of maize: Emergence and three-leaf stage," *Agricult. Forest Meteorol.*, vols. 174–175, pp. 65–84, Jun. 2013.

[21] K. Hufkens, E. K. Melaas, M. L. Mann, T. Foster, F. Ceballos, M. Robles, and B. Kramer, "Monitoring crop phenology using a smartphone based near-surface remote sensing approach," *Agricult. Forest Meteorol.*, vol. 265, pp. 327–337, Feb. 2019.

[22] Y. Zhu, Z. Cao, H. Lu, Y. Li, and Y. Xiao, "In-field automatic observation of wheat heading stage using computer vision," *Biosyst. Eng.*, vol. 143, pp. 28–41, Mar. 2016.

[23] W. Guo, T. Fukatsu, and S. Ninomiya, "Automated characterization of flowering dynamics in rice using field-acquired time-series RGB images," *Plant Methods*, vol. 11, no. 1, p. 7, 2015, doi: 10.1186/s13007-015-0047-9.

[24] X. D. Bai, Z. Cao, and L. Zhao, "Rice heading stage automatic observation by multi-classifier cascade based rice spike detection method," *Agricult. Forest Meteorol.*, vol. 259, pp. 260–270, Sep. 2018.
[25] J. Han, L. Shi, Q. Yang, K. Huang, Y. Zha, and J. Yu, "Real-time detection of rice phenology through convolutional neural network using handheld camera images," *Precis. Agricult.*, vol. 22, no. 1, pp. 154–178, Feb. 2021.
[26] M. Á. Castillo-Martínez, F. J. Gallegos-Funes, B. E. Carvajal-Gámez, G. Urriolagoitia-Sosa, and A. J. Rosales-Silva, "Color index based thresholding method for background and foreground segmentation of plant images," *Comput. Electron. Agricult.*, vol. 178, Nov. 2020, Art. no. 105783.
[27] G. E. Meyer and J. C. Neto, "Verification of color vegetation indices for automated crop imaging applications," *Comput. Electron. Agricult.*, vol. 63, no. 2, pp. 282–293, Oct. 2008.
[28] L. Zheng, J. Zhang, and Q. Wang, "Mean-shift-based color segmentation of images containing green vegetation," *Comput. Electron. Agricult.*, vol. 65, no. 1, pp. 93–98, Jan. 2009.
[29] H. Yin, Y. Chai, S. X. Yang, and G. S. Mittal, "Ripe tomato detection for robotic vision harvesting systems in greenhouses," *Trans. ASABE*, vol. 54, no. 4, pp. 1539–1546, 2011.
[30] J. L. Wang, *Research on Machine Vision Algorithm for Field Leaf Image Segmentation and Single 3D Reconstruction*. Beijing, China: China Agricultural Univ., 2013.
[31] C. Niu, H. Li, and Y. G. Niu, "Segmentation of cotton leaves based on improved watershed algorithm," *Comput. Electron. Agricult.*, vol. 478, pp. 425–436, Sep. 2016.
[32] D. G. Lowe, "Distinctive image features from scale-invariant keypoints," *Int. J. Comput. Vis.*, vol. 60, no. 2, pp. 91–110, Nov. 2004.
[33] N. Dalal and B. Triggs, "Histograms of oriented gradients for human detection," in *Proc. IEEE Comput. Soc. Conf. Comput. Vis. Pattern Recognit. (CVPR)*, Jun. 2005, pp. 886–893.
[34] N. Radakovich, M. Nagy, and A. Nazha, "Machine learning in haematological malignancies," *Lancet Haematology*, vol. 7, no. 7, pp. 541–550, 2020.
[35] I. Goodfellow, Y. Bengio, and A. Courville, *Deep Learning*. Cambridge, MA, USA: MIT Press, 2016.
[36] P. K. Sethy, N. K. Barpanda, A. K. Rath, and S. K. Behera, "Deep feature based rice leaf disease identification using support vector machine," *Comput. Electron. Agricult.*, vol. 175, Aug. 2020, Art. no. 105527.
[37] P. K. Sethy, N. K. Barpanda, A. K. Rath, and S. K. Behera, "Nitrogen deficiency prediction of rice crop based on convolutional neural network," *Ambient Intell Hum. Comput*, vol. 11, pp. 5703–5711, Nov. 2020, doi: 10.1007/s12652-020-01938-8.
[38] N. Codella, M. Moradi, M. Matasar, T. Sveda-Mahmood, and J. R. Smith, "Lymphoma diagnosis in histopathology using a multi-stage visual learning approach," *Proc. SPIE*, vol. 9791, Mar. 2016, Art. no. 97910H.
[39] J. Ryu, H. I. Koo, and N. I. Cho, "Word segmentation method for handwritten documents based on structured learning," *IEEE Signal Process. Lett.*, vol. 22, no. 8, pp. 1161–1165, Aug. 2015.
[40] Y. Wu, Z. H. Liu, X. F. Zhou, and Y. C. Zhang, "Aluminum casting type recognition based on texture features and SVM classifier," *Comput. Syst. Appl.*, vol. 27, no. 8, pp. 285–289, 2018.
[41] S. C. Long and L. J. Yao, "Stroke length texture features applied to intestinal cancer pathology picture recognition," *J. Zhejiang Univ. Technol.*, vol. 43, no. 1, pp. 110–114, 2015.
[42] Z. Z. Yang, N. Kuang, L. Fan, and B. Kang, "A review of image classification algorithms based on convolutional neural networks," *Signal Process.*, vol. 34, no. 12, pp. 1474–1489, 2018.
[43] Y. Bengio, A. Courville, and P. Vincent, "Representation learning: A review and new perspectives," *IEEE Trans. Pattern Anal. Mach. Intell.*, vol. 35, no. 8, pp. 1798–1828, Aug. 2013.
[44] P. Wang, E. Fan, and P. Wang, "Comparative analysis of image classification algorithms based on traditional machine learning and deep learning," *Pattern Recognit. Lett.*, vol. 141, pp. 61–67, 2021.
[45] D. M. Woebbecke, G. E. Meyer, K. Von Bargen, and D. A. Mortensen, "Color indices for weed identification under various soil, residue, and lighting conditions," *Trans. ASAE*, vol. 38, no. 1, pp. 259–269, 1995.
[46] T. Y. Zhang and C. Y. Suen, "A fast parallel algorithm for thinning digital patterns," *Commun. ACM*, vol. 27, no. 3, pp. 236–239, Mar. 1984.
[47] W. Tang, J. Hu, and H. Zhang, "Kappa coefficient: A popular measure of rater agreement," *Gen. Psychiatry*, vol. 27, no. 1, p. 62, 2015.

YUANQIN ZHANG received the dual bachelor's degree in engineering and science from the Hubei University of Science and Technology, China, in 2016. She is currently pursuing the Ph.D. degree from the College of Mathematics Informatics, South China Agricultural University, China. Her research interest includes image processing in agriculture.

DEQIN XIAO received the Ph.D. degree. She is currently working with the College of Mathematics and Informatics, South China Agricultural University. She is Ph.D., Professor, doctoral supervisor, deputy director of Guangdong Agricultural Breeding IoT engineering technology center, director of Scau Agricultural big data engineering center. She has hosted for more than ten software copyright registration, obtained one patent of invention, three utility patents, and three invention patents are opening, published more than 80 articles, with which EI indexes more than 30 and SCI indexes 50. Her research interests include video big data analysis, software design and development, agriculture IoT, and other scientific research and application promotion.

YOUFU LIU received the M.S. degree from the College of Engineering, South China Agricultural University, Guangzhou, China, in 2019, where he is currently pursuing the Ph.D. degree with the College of Mathematics and Informatics. His research interests include computer vision and precision agriculture.